11th International Symposium on Turbulence and Shear Flow Phenomena (TSFP11)
Southampton, UK, July 30 to August 2, 2019

ON COHERENT STRUCTURES PRODUCED BY A VORTEX-GENERATOR LOCATED UPSTREAM OF A RAMP

M. A. Mohamed

School of Mechanical and Aerospace Engineering
Nanyang Technological University
50 Nanyang Ave, Singapore 639798
mohd.arif@ntu.edu.sg

A. U. Cheawchan

School of Mechanical and Aerospace Engineering
Nanyang Technological University
50 Nanyang Ave, Singapore 639798
atchauea001@e.ntu.edu.sg

Z. W. Teo

School of Mechanical and Aerospace Engineering
Nanyang Technological University
50 Nanyang Ave, Singapore 639798
alvinteozw@ntu.edu.sg

T. H. New

School of Mechanical and Aerospace Engineering
Nanyang Technological University
50 Nanyang Ave, Singapore 639798
dthnew@ntu.edu.sg

B. F. Ng

School of Mechanical and Aerospace Engineering
Nanyang Technological University
50 Nanyang Ave, Singapore 639798
bingfeng@ntu.edu.sg

ABSTRACT

The present study investigates the coherent flow structures and behaviour produced by a vortex-generator (VG) positioned on a flat-surface upstream of a 20° downwards inclined ramp. The effects of the distance between the VG and the ramp, as well as its orientation with respect to the free-stream direction, are also studied as part of the overall understanding. Surface oil flow visualizations, as well as Large-Eddy Simulations (LES) based on ANSYS FLUENT were conducted and their results compared. The former reveals qualitatively that a 30° skewed VG leads to significant flow blockage and differences between the flow structures produced by each of the VG plates. Simulation results further show that for the 30° skewed VG, the left VG plate leads to significant vortex-shedding behaviour while producing a weak streamwise vortex, due to its higher flow blockage. On the other hand, the right VG plate produces only a weak streamwise vortex due to its much lower flow blockage. Coupled with the downwards inclined ramp, these flow structures and their mutual interactions result in rapid transition to turbulence.

INTRODUCTION

Effective flow control of the airflow around helicopter fuselages to mitigate could lead to reduced fuel consumption and better flight controls of these highly complex rotorcrafts. While different approaches had been mooted to achieve that, passive devices such as vortex generators (VGs) remain one of the more cost-effective, robust and simpler possible solutions. They are known to re-energize the boundary layer via streamwise vortices produced by the vortex generators, thereby delaying or preventing separation from solid boundaries. It should be noted that one of locations along a helicopter fuselage where flow separations are significant is the helicopter ramp region at the lee-side of the fuselage. The ramp is typically inclined at a significant angle when closed during flights and that tends to lead to heightened drag levels. While the effects of VGs upon flat solid boundaries parallel to the free-stream direction have been well-studied and understood (Lin, 2002, Godard and Stanislas, 2006) the same may not be said for VGs meant to reduce flow separations caused by the presence of a ramp.

With this in mind, it would then be worthwhile to study the evolution and behaviour of the resulting streamwise vortices in the presence of a simplified moderately inclined ramp. In some ways, the flow configuration is somewhat similar to a backward-facing step problem, albeit one with a non-zero inclination angle. This problem is by itself non-trivial given the fact that in real-life, varying the angle-of-incidence of a helicopter would bring about even more complex airflows around the fuselage and ramp regions. For example, at low positive angles-of-incidence, stable vortices would persist along the ramp region. In contrast, negative angles-of-incidence would result in the vortices being shed upstream of the ramp (Mistry and Lamb, 1980). Introducing VGs to this part of the flow would provide an interesting perspective into the interactions of VG-induced streamwise vortices with the ones that are already existing. Hence, the present study attempts to shed more light upon these flow interactions and subsequent behaviour.

EXPERIMENTAL SETUP AND PROCEDURES

The experiments were conducted in a closed-loop wind tunnel with a test section measuring 0.72m (H) × 0.78m (W) × 2m (L), where a free-stream velocity of 50m/s and a turbulence intensity of approximately 2% was used. A simplified Plexiglas-based ramp model was constructed out of a 1000 mm flat wall combined with a 20° downwards-inclined ramp and located within the wind tunnel test section. The VG was based on two rectangular plates of 62 mm (L_{VG}) × 19.2 mm (H_{VG}) and was located at $5H_{VG}$ upstream of the sharp ramp transition.

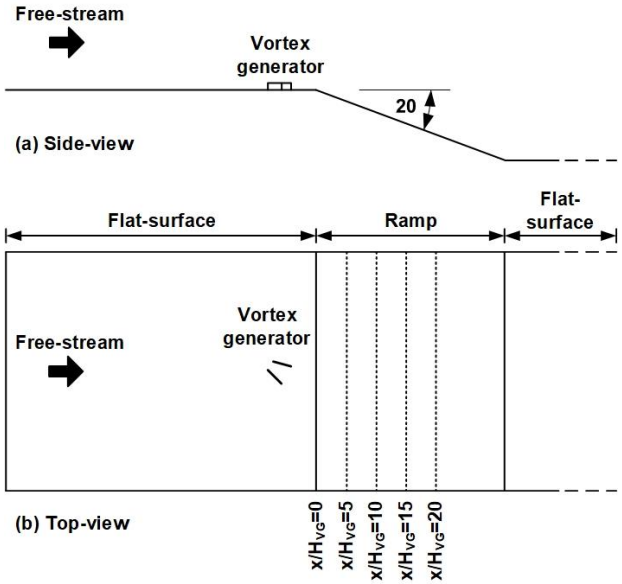

Figure 1 Schematics of the experimental/simulation setups and locations of the cross-sectional planes where further results were extracted.

The included angle between the two VG plates is 30°. Two VG alignments were studied here - θ=0° and 30° with respect to the free-stream direction and schematics of the experimental and simulation setups are shown in Fig. 1. The figure also shows how the VG appears when it is aligned in the θ=30° orientation and locations where cross-sectional results from the numerical simulations are extracted for further analysis later.

For surface oil flow visualizations, a fine suspension of pigment was mixed with mineral oils and coated upon the ramp test model to observe the resulting flow streaks for a qualitative understanding. Fluorescent zinc sulphide pigment was used, while the mineral oils comprised of white oil and CarlubeT^{M} oil. A digital single-lens-reflex (DSLR) camera remotely-controlled by a workstation was subsequently used to capture the surface oil flow patterns after the flow patterns had reached a steady state after approximately 5-10 minutes of wind tunnel run-time, depending on the exact test configuration.

NUMERICAL PROCEDURES

The computational domains for the skewed and symmetric VG cases consisted of 74,227,778 and 94,212,365 nodes respectively. The generated grids are of polyhedral proportions as polyhedral cells predict accurate gradients given that they have many neighbouring cells (with the appropriate linear shape functions). No-slip surfaces are layered with 40 prismatic cells to account for the boundary layer. The simulations were performed in ANSYS FLUENT^{TM} 18.1. The fractional step velocity-coupling scheme with non-iterative time advancement (NITA) was adopted for the LES. Gradients were computed using the Least Square Cell Based method. Spatial discretization for pressure and velocity were based on second order and bounded central differencing respectively. The LES model chosen for this simulation was the Dynamic Smagorinsky-Lilly (Germano et al., 1991).

Velocity fields were first simulated with Reynolds-Averaged Navier-Stokes (RANS) approach and used as initial flow conditions for subsequent LES. This was performed using the Spalart-Allmaras turbulence model, chosen primarily here for its well-known capabilities in predicting external flows

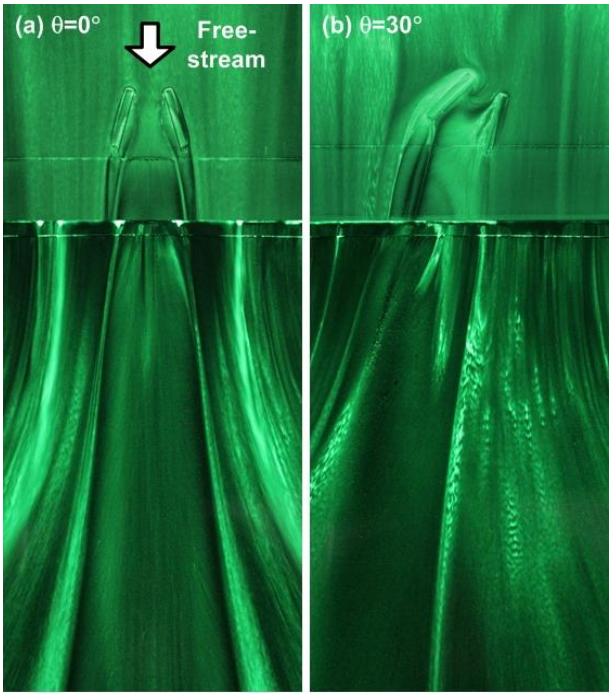

Figure 2 Surface oil flow visualizations taken for the rectangular VG aligned at (a) θ=0° and (b) θ=30° to the free-stream direction.

reasonably well at a lower computational cost. The velocity profile at the inlet followed the 1/7th power-law with a freestream velocity of 50m/s. The turbulent boundary layer at the inlet was set at 20mm, as obtained earlier from particle-image velocimetry experiments. For the RANS simulations, a turbulence intensity of 2% was prescribed at the inlet. For the LES, time-dependent velocity perturbations at the inlet were generated using the Vortex Method. This is to negate weak correlations otherwise seen with random perturbations which would see turbulence dissipate far too quickly.

RESULTS AND DISCUSSION

Firstly, surface oil flow visualization results will be presented in Figure 2 for a first-hand appreciation of the flow scenarios encountered here, where the VG was configured to be aligned with the free-stream at θ=0° and 30°. The surface oil patterns will provide some qualitative information on the behaviour of the streamwise vortices produced by the VG under different test configurations. Note that all images were taken with the camera axes aligned perpendicularly to the flat-surface and ramp.

As expected, the results show that when the VG is aligned parallel with the free-stream (i.e. θ=0° as shown in Figure 2(a)), the surface oil patterns reveal the imprints associated with a pair of symmetrical streamwise vortices originating from the VG. In addition, spread-rate of the streamwise vortices "legs" appear to be higher when they are above the ramp as compared to that above the flat-surface, though this will have to be ascertained further. When the VG is skewed at an angle of θ=30° as shown in Figure 2(b), it is clear that the resulting streamwise vortices becomes highly skewed with respect to the free-stream direction as well. Closer inspection of the figure will show a highly asymmetric flow field surrounding the 30° skewed VG as it encountered the free-stream. In particular, surface oil patterns along the flat-surface indicate that, as a

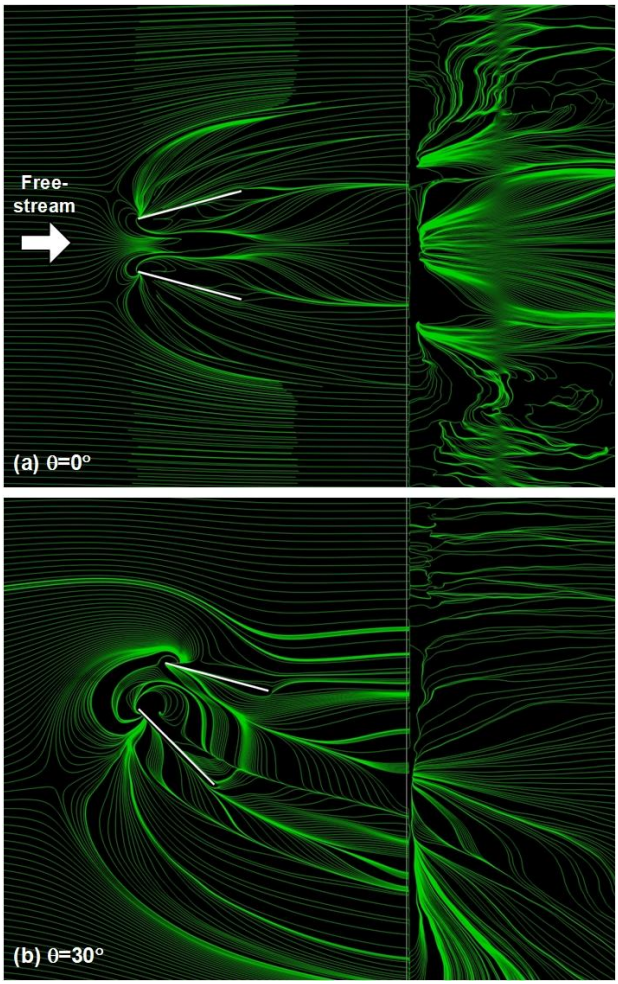

Figure 3 Limiting streamlines extracted from numerical simulations for (a) θ=0° and (b) θ=30° aligned VG.

direct result of the significant VG skewness, the left VG plate produces a much higher blockage to the free-stream while the opposite is true for the right VG plate. As result, much more drastic flow separation behaviour is expected to be produced by the left VG plate. In contrast, a more gradual flow separation behaviour is expected to be produced by the right VG plate. This notion is further reinforced by the surface oil patterns along the ramp, where the left vortex-core of the asymmetric streamwise vortices appears to leave a significant larger imprint than the right vortex-core. Additionally, it should be noted that the streamwise vortices remain skewed along the ramp surface just as they are along the flat-plate, at least within the imaging window here.

As the surface oil patterns only reveal the imprints of the streamwise vortices convecting about the flat-surface and ramp and lacks additional details, LES results will now be presented to clarify the flow fields further. Firstly, limiting streamlines extracted from the simulations and shown in Fig. 3 reveal additional flow intricacies on top of the oil streak patterns. The gross patterns between the experiments and simulations agree reasonably well, where symmetrical flow separations about the VG at θ=0° alignment can be seen to produce streamwise vortices that rotate about their cores, which in turn produce limiting streamlines that spiral along the flat-surface. What is more interesting are the flow details indicated by the limiting streamlines along the ramp surface, where the disruptions to the

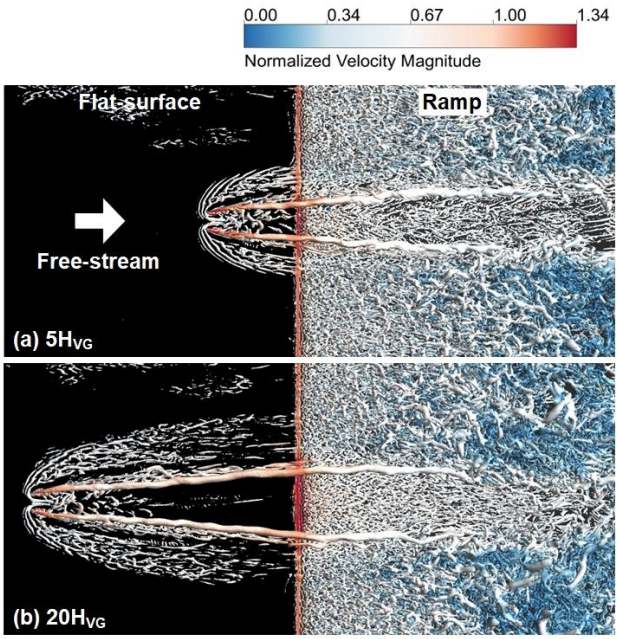

Figure 4 Top-views of the streamwise vortices produced by the VG when located at (a) 5H$_{VG}$ and (b) 20H$_{VG}$ upstream of the ramp.

characteristics of the streamwise vortices can be discerned. In this case, the presence of a sharp flat-surface-ramp interface appears to lead to its interactions with the streamwise vortices, as well as additional flow interactions between the streamwise vortices and the ramp boundary layer. At θ=30°, the flow separations associated with the VG become significantly more complex, with a multitude of flow structures formed. The flow field becomes highly asymmetric where the separated flow from the left VG plate is significantly more dominant that that produced by the right VG plate. Additionally, the high flow blockage posed by the left VG plate is apparent and its skewing of the free-stream, even over the ramp surface, can be observed readily.

Secondly, the influence of the VG location with respect to the start location of the ramp was investigated by comparing the resulting flow fields and structures associated with the VG located at 5H$_{VG}$ and 20 H$_{VG}$ distances upstream of the ramp, as shown in Fig. 4. Note that the flow structures are identified based on λ_2 vortex criterion and colour-tagged by normalized velocity magnitudes. It can be discerned clearly from the figure that the VG location plays an important role in terms of the persistence of the resulting streamwise vortices over the ramp surface. Specifically, streamwise vortices produced by the VG at 20H$_{VG}$ location do not persist as far along the ramp surface as those produced by the VG at 5H$_{VG}$ location. For effective flow separation control over the ramp region, the streamwise vortices should remain coherent and persist for as far downstream as possible. With this in mind, subsequent LES results shown will be for VGs located at 5H$_{VG}$ location only.

Figure 5 shows 3D views of the flow structures associated with the flow scenario without any VGs, as well as VGs aligned at θ=0° and 30° configurations. For the scenario without any VGs as depicted in Fig. 5(a), no coherent structures can be observed to form. Instead, turbulent flow structures are formed along the ramp surface as a result of the flow separation at a relatively high Reynolds number. When

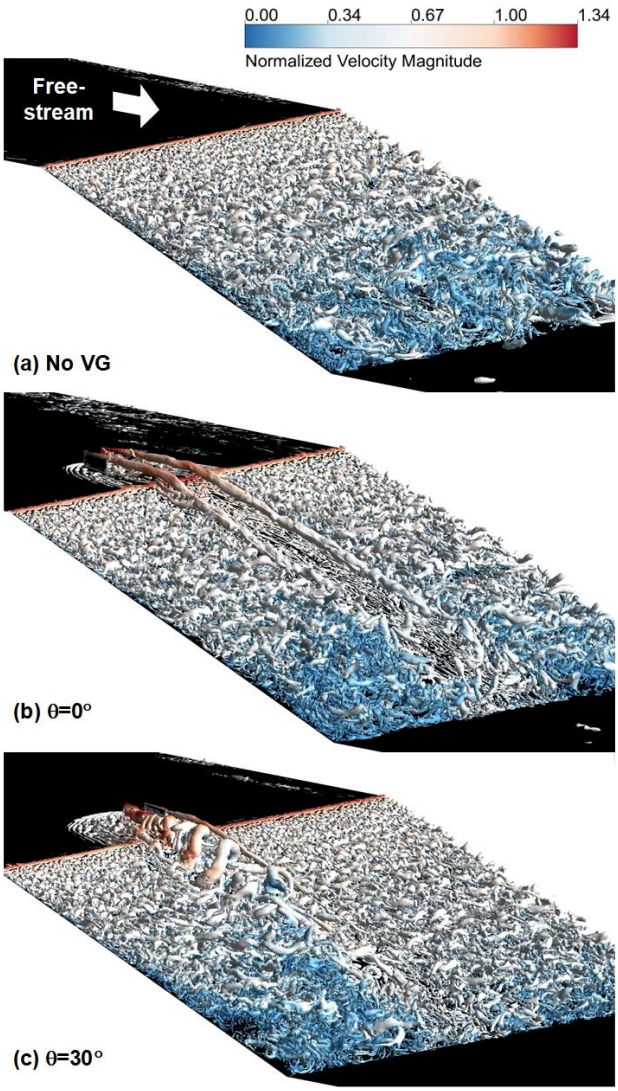

Figure 5 3D views of the flow structures resulting from (a) no VG configuration, as well as VG skewed at (b) θ=0° and (c) θ=30°, as identified by λ_2 vortex criterion and colour-tagged by normalized velocity magnitudes.

the VG is used and aligned at θ=0° as shown in Fig. 5(b), a pair of coherent streamwise vortices can clearly be observed to emanate from the VG. The "legs" of the streamwise vortices can be seen to follow the inclination of the ramp, though they remain at some distance above it. Unlike what is typically seen for such streamwise vortices along a purely flat-surface, the streamwise vortices here do not persist very far above the ramp surface before they transit into incoherence. As for the θ=30° aligned VG shown in Fig. 5(c), it is clear that it does not produce coherent streamwise vortices typically associated with the use of VGs. Instead, regular shedding of coherent vortices appears to be produced by the left VG plate, while the right VG plate produce a vortex filament similar to those observed in Fig. 5(b) but significantly slenderer and less persistent.

Figure 6 shows the same three flow scenarios but from the top-view, so as to supplement observations gathered from Fig. 5. In particular, the differences between the flow behaviour structures produced by the left and right VG plates as shown in Fig. 6(c) become much clearer. Firstly, the significant blockage caused by the left VG plate leads to significant

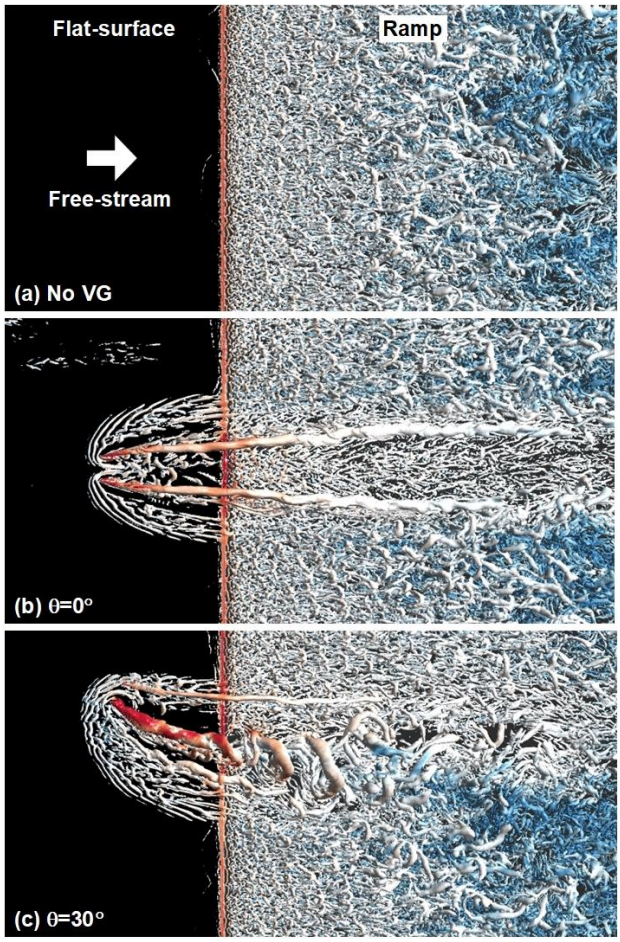

Figure 6 Top-views of the flow structures resulting from (a) no VG configuration, as well as VG skewed at (b) θ=0° and (c) θ=30°, as identified by λ_2 vortex criterion and colour-tagged by normalized velocity magnitudes.

formation of horseshoe-like structures upstream of it, where they wrap around it asymmetrically. This is in stark contrast to the right VG plate, where formation of horseshoe-like vortices ahead of it is more moderate. Furthermore, it is worth noting that the streamwise vortex produced by the right VG plate is visually smaller and weaker than those produced by the θ=0° aligned VG, and that its trajectory is more parallel with the free-direction as it convects aft of the right VG plate. More importantly, the rotational sense of the streamwise vortex produced by the right VG plate appears to be clockwise when viewed from a downstream location, opposite to that of the θ=0° configuration. However, a closer inspection of the figure will show that the right VG plate at θ=30° becomes orientated in the opposite direction as compared to that at θ=0°. Hence, it should not be surprisingly to observe this difference in the rotational sense. To clarify this further, Fig. 7 shows close-up views of the θ=0° and 30° aligned VGs, where the flow structures produced by them can be better discerned.

Since Figs. 5(c) and 6(c) have demonstrated the significantly different vortex systems produced by the left and right VG plates, it will be interesting to inspect them closer as they gradually convect downstream. For conventional θ=0° aligned rectangular VGs such as the one shown in Figs. 5(b) and 6(b), it should be intuitive that cross-sectional views of the streamwise vortices would reveal two approximately

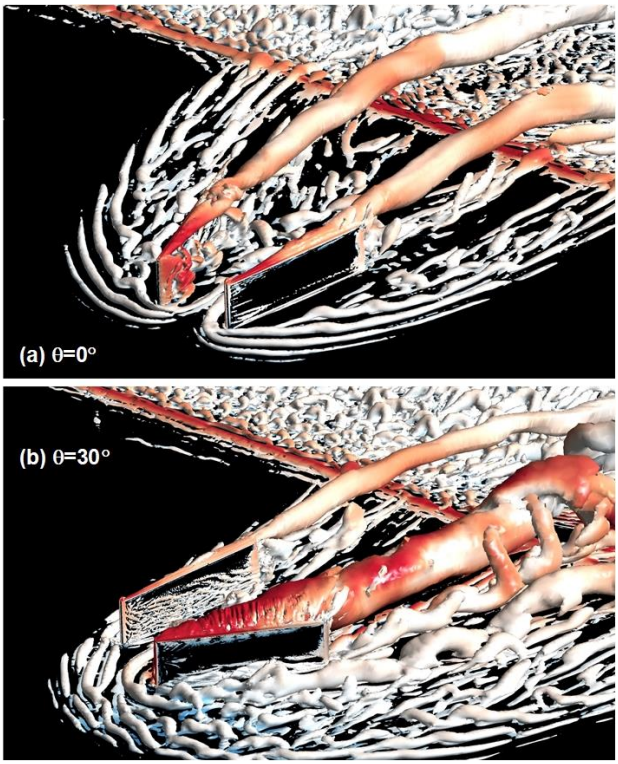

Figure 7 Close-up views of the coherent flow structures produced by the VG aligned at θ=0° and 30°

symmetrical counter-rotating vortex-cores about their symmetry plane until they dissipate through viscous effects. To validate this, Fig. 8 shows the five corresponding cross-sectional vorticity results for the θ=0° configuration at x/H_{VG}=0, 5, 10, 15 and 20 locations. It should be noted that the first plane coincides exactly with the transition from the flat-surface to the ramp and subsequent planes are located progressively downstream along the ramp. From the figure, it can be seen that a fairly symmetric pair of streamwise vortices is produced, where it persists till x/H_{VG}=20 before interactions with the ramp boundary layer and viscous effects render it incoherent.

For the θ=30° aligned rectangular VGs however, the cross-section views of the vortex systems are expected to be quite different, as shown in Fig. 9. The cores of the vortex systems produced by the VG can be discerned quite clearly at x/H_{VG}=0. Therefore, while Figs. 5(c) and 6(c) shows regular shedding of vortices from the left VG plate, it nevertheless generates a clockwise rotational-sense streamwise vortex as well. As postulated earlier, the rotational sense of the vortex produced by the right VG plate is indeed in the clockwise direction. Their qualitative sizes are quite different however, with the left VG plate producing a qualitatively larger vortex-core. As the location moves progressively more downstream, the coherence of the streamwise vortex produced by the left VG plate reduces drastically, presumably a result of the flow separation vortices interacting with the it. More importantly, interactions between the above-mentioned streamwise vortex, flow separation vortices and the ramp boundary layer appear to lead to detrimental flow effects. For instance, significant fluid ejections away from the near-wall region can be observed at x/H_{VG}=15 and 20 locations, which could potentially lead to worse-than-expected flow separation control by the VG.

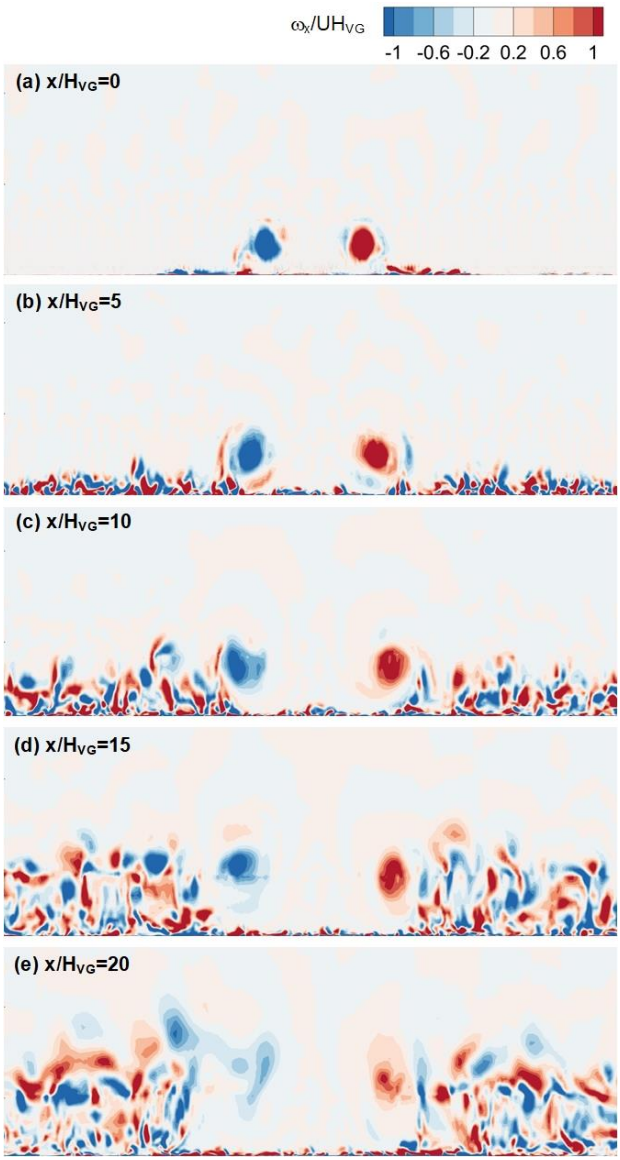

Figure 8 Cross-sectional vorticity distributions taken downstream of the θ=0° aligned VG.

At this point, the preceding results indicate that the use of VGs for the purpose of flow separation control associated with a flat-surface-ramp setup appears to be feasible. However, there are certain take-aways from the present study, as revealed by the experimental and simulation results: Firstly, the VG should be located upstream but closer to the start of the ramp. While the present study did not explore whether there is an optimal location to position the VG, it would appear that the VG should be located such that the streamwise vortices that it produces have sufficient distance/time to develop before they encounter the ramp and any adverse pressure gradient associated with it. Secondly, off-designed VGs such as those that are skewed relatively to the free-stream, could quite possibly be detrimental to the flow-separation control effects typical associated with VGs. On top of that, they would also likely lead to higher pressure drag, potentially adverse flow interactions between the significantly different vortex structures produced by each of the VG plates, as well as less predictable flow characteristics. Hence, the use of off-designed VGs or VGs in off-design conditions (i.e. cross-wind

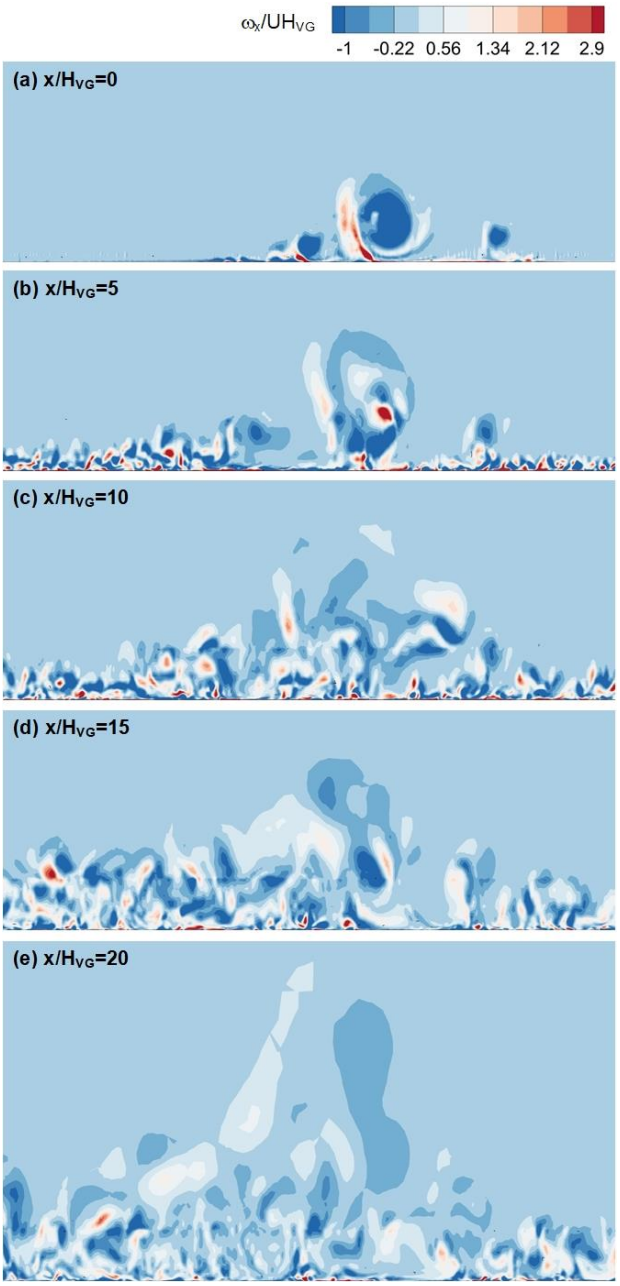

Figure 9 Cross-sectional vorticity distributions taken downstream of the θ=30° aligned VG.

conditions) will have to be carefully investigated prior to their implementations and usages.

CONCLUSIONS

An experimental and numerical study had been conducted on the use of a rectangular VG upon a ramp setup, where effects of its upstream location and skewness relative to the free-stream direction have been investigated. Both experimental oil streak pattern and simulation limiting streamline results show the drastic effects of VG skewness upon the wall shear distributions and the vortex structures produced. In particular, it is observed that a 30° skewed VG leads to highly asymmetric flow structures emanating from the VG plates, due to the significantly different flow blockages posed by each of these VG plates. For the one with a high flow blockage, regular vortex-shedding occurs on top of a qualitatively stronger and larger streamwise vortex. In contrast, the one with a smaller flow blockage produces only a weak streamwise vortex with no vortex-shedding. In fact, this streamwise vortex possess a rotational sense opposite to that when the VG is aligned at θ=0°. However, it should also be noted that these flow outcomes are dependent upon the exact VG geometry and skew angle. Lastly, the streamwise vortices produced by the present skewed VG do not persist as far downstream as those produced by the non-skewed VG. For a ramp setup such as the one investigated within the present study, the results support the notion that VGs aligned with the free-stream and ramp direction are likely to work better than those that are non-aligned. Furthermore, off-designed VGs or VGs deployed in off-design conditions may significantly mitigate flow-separation control effectiveness.

ACKNOWLEDEMENTS

The authors acknowledge the support for the study by Leonardo Company and Nanyang Technological University (NTU). Support for the second author through an NTU PhD Research Scholarship is also kindly acknowledged.

REFERENCES

Betterton, J.G., Hackett, K.C., Ashill, P.R., Wilson M.J., Woodcock, I.J., Tilman, C.P. and Langan, K.J., 2000, "Laser Doppler Anemometry Investigation on Sub-Boundary Layer Vortex Generators for Flow Control", *10th International Symposium on Applications of Laser Techniques to Fluid Mechanics*, *pp*. 10-13

Germano, M., Piomelli, U., Moin, P., & Cabot, W. H., 1991, "A Dynamic Subgrid-scale Eddy Viscosity Model", *Physics of Fluids A: Fluid Dynamics*, Vol. *3, pp. 1760-1765*

Godard, G. and Stanislas, M., 2006. "Control of a Decelerating Boundary Layer. Part 1: Optimization of Passive Vortex Generators", *Aerospace Science and Technology*, *10*(3), *pp*.181-191.

Jeong, J., & Hussain, F., 1995, "On the Identification of a Vortex", *Journal of Fluid Mechanics, 285*(*1), pp*. 69-94.

Kwon, O. K., and Pletcher, R. H., 1981, "Prediction of the Incompressible Flow Over a Rearward-Facing Step", *Technical Report HTL-26, CFD-4*, Iowa State Univ., Ames, IA

Lin, J. C., 2002, "Review of Research on Low-Profile Vortex Generators to Control Boundary Layer Separation", *Progress in Aerospace Sciences*, Vol. 38, *pp*. 389-420

Menter, F. R., Langtry, R. B., Likki, S.R., Suzen, Y.B., Huang, P. G. and Volker, S., 2006, "A Correlation-based Transition Model Using Local Variables—Part I: Model Formulation", *Journal of Turbomachinery, 128(3), pp*. 413-422

Mistry, H. and Lamb, R., 1980, "An Investigation of Drag Associated with the Upswept Rear Fuselage of a Helicopter", *University of Bristol, Aero Engineering Report* No. 257